Improving Inductive Sensing of Superparamagnetic Nanoparticles through Orientation of Easy Axes

Margo Hauwaert
ICTEAM
UCLouvain
Belgium
margo.hauwaert@uclouvain.be

Nordin Trifiro
ICTEAM
UCLouvain
Belgium

Vanessa Pilati
Dpt Fis. Applicada
Universidad de Oviedo
Spain

Louise Lejeune
IMMC
UCLouvain
Belgium

Simo Spassov
Geophysics Dpt
IRM-KMI
Belgium

Martin Lefebvre
EEMCS
TU Delft
The Netherlands

Ramy Moumneh
ICTEAM
UCLouvain
Belgium
ramy.moumneh@uclouvain.be

Sophie Hermans
IMMC
UCLouvain
Belgium
sophie.hermans@uclouvain.be

Montserrat Rivas
Dpt. Fis. Applicada
Universidad de Oviedo
Spain
rivas@uniovi.es

Jean-Pierre Raskin
ICTEAM
UCLouvain
Belgium
jean-pierre.raskin@uclouvain.be

***Abstract*—Magnetic nanoparticles are being actively explored for diagnostic use in inductive biosensors, due to their high susceptibility and low hysteresis. In this work, we demonstrate how drying particles under a DC magnetic field within a membrane substrate affects sensitivity of the sensing platform. When the nanoparticles (Fe_3O_4, $CoFe_2O_4$, $MnFe_2O_4$) are dried within a static magnetic field parallel to the inductive AC sensing field, the sensor response is increased by 6 to 16 % depending on sample alloy and mass. Furthermore, when the drying field and excitation field are orthogonal, the signal is decreased by similar factors. The results point to a Brownian rotation of the particles during the drying process.**

***Index Terms*—superparamagnetic nanoparticles, inductive sensing, anisotropy constants, magnetic biosensors, easy axis**

I. Introduction

Magnetically anisotropic materials have an easy axis (EA), determined by physical shape and crystal structure, which is the energetically preferred direction of the spontaneous magnetization vector. When ferro- or ferrimagnetic materials are reduced to 10-20 nm, their magnetic anisotropy energy becomes so small that the thermal energy at room temperature is sufficient to overcome the energy barrier separating two opposite orientations of the magnetization vector. As a result, these two orientations become equally probable and the net magnetization, averaged over the observation time window, becomes zero in the absence of an external field. This null remanence resembles the paramagnetic state, but the nanomaterial retains the high saturation magnetization characteristic of ferromagnets. Hence the term 'superparamagnetic', a magnetic behavior which only happening in nanoscale ferro(i)magnetic materials. The small size, zero coercivity, and large saturation magnetization make these nanoparticles ideal for both in vivo and in vitro biomedical applications. [1] In biosensors, they can be efficient labels for biomolecules due to their tunable size and surface chemistry, and are used e.g. in quantitative immuno-sensors such as lateral flow assays (LFAs) whose best examples are pregnancy selftests. Moreover, one can use their magnetism for pre-concentration or separation of the target analyte from the biological fluid, increasing detection sensitivity and specificity [2]. In practical applications, Superparamagnetic Nanoparticles (SPNs) can be subjected to DC magnetic fields of several thousands of Oersteds for motion, concentration or transduction purposes. When they're free to rotate, this results in an alignment of their EA by Brownian rotation [4]. Theoretical models are insufficient to fully predict their magnetic response in complex biological systems due to surface effects and clustering [3]. The orientation of SPNs has mainly been studied for hyperthermia applications. It was found that the exposure of a group of magnetite Fe_3O_4 SPNs within a cell-like environment creates chain-like structures, affecting the shape anisotropy and the relaxation time [5]. The imaginary susceptibility is increased, resulting in more efficient heat dissipation [6]. However, the effects of nanoparticle pre-orientation on the real part of complex susceptibility are less investigated but equally important in inductive sensing applications. Martin et al. [1] found that when the EA were oriented parallel to the sensing field, Zeeman energy and anisotropy contributions cooperate, resulting in a directional susceptibility increased with roughly 10 %. When EA were transverse to sensing field, susceptibility was decreased by roughly 10 %.

In this work, we study how SPN alignment affects the directional susceptibility and can be used to improve sensor sensitivity. More specifically, we investigate how pre-aligning SPNs can improve the signal-to-noise ratio (SNR) for inductive nanoparticle detection in porous substrates. SPNs are dispensed on nitrocellulose membranes, mimicking magnetic LFAs, in the absence or presence of an external static magnetic field. In the absence of such a drying field, the SPNs are shown

M. Hauwaert is a FRIA grantee of the Fonds de la Recherche Scientifique - FNRS. The authors acknowledge financial support from the Ministry of Science and Innovation of the Spanish Government under grant PLEC2022-009490

2025 IEEE SENSORS | 979-8-3315-4467-6/25/$31.00 ©2025 IEEE | DOI: 10.1109/SENSORS59705.2025.11330555

to have randomly distributed EA. Conversely, when the drying occurs under a static magnetic field $\overrightarrow{H_z^D}$, the nanoparticles experience a torque that reorients their EA along the direction of the external field (Brownian motion). Upon completion of the drying process, the SPNs become immobilized within the nitrocellulose matrix, preserving the alignment of their EA. As summarized in Fig. 1, we assess the consequences for inductive sensing with planar and tubular coils, which generate an excitation field respectively parallel ($\overrightarrow{H_z^E}$) and orthogonal ($\overrightarrow{H_y^E}$) to the external field imposed during drying. Three types of SPNs with varying magnetocrystalline anisotropies are studied: 10.1 nm magnetite Fe_3O_4, 8.9 nm $MnFe_2O_4$ and 11.1 nm $CoFe_2O_4$ SPNs.

II. Materials and Methods

A. Superparamagnetic Nanoparticle Synthesis

Spinel ferrites ($M^{2+}Fe_2^{3+}O_4$) containing 3d metals allow for excellent fine-tuning of magnetic properties. $MnFe_2O_4$, $CoFe_2O_4$ and Fe_3O_4 nanoparticles were previously synthesized according to the co-precipitation method and functionalised with citric acid as described in [7]. Table I displays the nanoparticle average diameters D (obtained by transmission electrode microscope images) as well as the bulk magnetocrystalline anisotropy constants K_m and the specific saturation magnetisation M_s at room temperature [8].

TABLE I
Properties at 300 K of Nanoparticles Used in Experiments

Alloy	D (nm)	$M_s\left(\frac{\mathrm{Am^2}}{\mathrm{kg}}\right)$	$K_m\left(\frac{\times 10^4 \mathrm{J}}{\mathrm{m^3}}\right)$
$MnO \cdot Fe_2O_3$	8.9	80	0.3
$CoO \cdot Fe_2O_3$	11.1	80	20
Fe_3O_4	10.1	91	1.2

B. Sample Preparation

Square sample of 7x7 mm were cut from polyester backed nitrocellulose CN95 (Sartorius, Germany). Volumes of 5.3 μl of different nanoparticle suspensions were pipetted onto them resulting in the different SPN masses in Fig. 3. This volume was chosen to avoid the coffee ring effect (excessive nanoparticle accumulation on the borders). Within 10 seconds after the liquid was applied, the square was either kept in a Petri dish ('no field drying'), or put in a 500 mT C-core magnet ('field drying'), as represented by the table columns in Fig. 1.

C. Measurement Protocol

Both inductive sensors have the same transduction principle: the presence of SPNs causes an increase in inductance which is measured as a decrease in oscillation frequency of the LC-tank sensor: $\Delta f \propto \frac{1}{\sqrt{\Delta L}}$ [9]. We define signal amplitude S as the the relative change in inductance without sample L_{empty} and with sample L_{sample}, normalized by the mass of nanoparticles within the sample m_{sample}:

$$S = \left\| \frac{L_{empty} - L_{sample}}{L_{empty}} \right\| \cdot \frac{100}{m_{sample}} \quad \left[\frac{\%}{mg}\right]$$

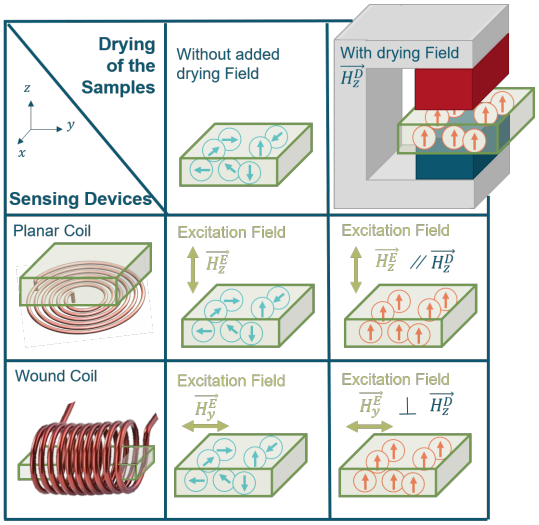

Fig. 1. Nanoparticles within nitrocellulose squares are either dried without or with external magnetic field, generated by a C-magnet of 0.5 T resulting in a non-arbitrary orientation of the easy axis. They are then measured in both a planar and wound coil. For the samples dried under field, this results in an excitation that is respectively parallel or transverse to the easy axis orientation. (Drawing not at scale)

Samples were inserted in the wound coil or positioned on the planar coil in a repeatable way. Each sample is added and removed at least eight times with a 30-seconds interval. As illustrated by the rows of Fig. 1, the samples were measured by two types of inductors with different conditioning chains.

a) Planar Detection Coil: An LDC 1614 'inductance to digital converter' was purchased from Texas Instruments. Two identical 8.5 μH planar coils with 38 turns each are implemented on this board, allowing differential detection and improved SNR. Indeed, one coil is exposed intermittently to the sample while the other stays empty during the whole measurement, serving as baseline for sensor drift. For samples dried under $\overrightarrow{H_z^D}$, this coil's excitation field $\overrightarrow{H_z^E}$ is parallel to the main EA orientation.

b) Wound Detection Coil: 18 turns of 480 μm copper wire were wound around a cylindrical PLA support. This 1.92 μH inductance is integrated with two 1 nF capacitances in a Colpitts oscillator, which oscillation frequency is read by a Teensy 4.1 microcontroller. Since this measurement is not corrected with a differential component and performed with a simpler interfacing circuit, the SNR is lower. For samples dried under $\overrightarrow{H_z^D}$, this coil's excitation field $\overrightarrow{H_y^E}$ is transverse to the main EA orientation.

III. Results

a) Aggregation: Since a detailed study of clustering dynamics of SPNs within membranes is not found at the start of this work, Fe_3O_4 SPNs were suspended within a glass fiber membrane, both without and with external field. For better visibility, we took 50 nm diameter rather than the 10.1 nm which is investigated further. Although 50nm is larger than the critical superparamagnetic diameter for magnetite, their

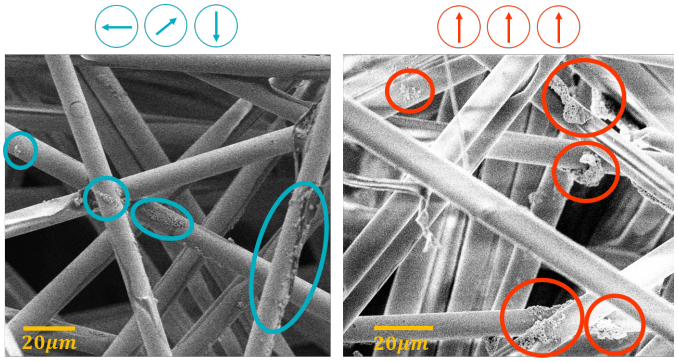

Fig. 2. SEM images of 50 nm magnetite nanoparticles dried in glass fiber membrane. When dried under field (resulting in aligned easy axis) the particles have a higher tendency to cluster.

coercivity is low enough and the external field high enough, to serve as an informative approximation. Scanning electron microscope (SEM) analysis on Fig. 2 reveals morphological differences between drying without and with static magnetic field. In the former, clusters are smaller and tend to be elongated along the fiber. In the latter, clusters are larger and can be orthogonal to the fiber direction. This cluster formation is similar to what was previously observed in agarose [5], suggesting that particles rotate before clustering.

b) EA Orientation: Figure 3 shows the signal amplitude expressed in % per nanoparticle mg for samples respectively measured with the planar and the wound coil. The wound coil has too low SNR for the 18.6 μg $CoFe_2O_4$ and 4.2 μg $MnFe_2O_4$ samples (given it is not in a differential system, while the planar coil is). First, a clear distinction exists between the signal amplitude caused by the three types of alloys, no matter the magnetisation or coil, which can be explained by the microcrystalline anisotropy constant K_m in Table I. For similar saturation magnetisation, K_m greatly affects the initial susceptibility χ_i: the lower K_m, the higher χ_i [7]. This explains why $MnFe_2O_4$ samples have the highest signal and $CoFe_2O_4$ the lowest. Second, drying the sample in a field parallel to the excitation field improves the signal amplitude by 6 to 16 % compared to sample dried without field, while it decreases the signal by 6 to 16 % in the transverse case. In all cases, the difference between sensing of the samples dried with and without external field is higher than two times the highest standard deviation.

c) Mobility: Drying under field is done by depositing a square of paper on a C-magnet : while on macro-scale the field is supposedly constant within the magnet gap, a field gradient can still exist across the membrane, which was hypothesized to cause vertical nanoparticle displacement through the 160 μm thick membrane, supposedly significant since the inductance change of the planar coil is very sensitive to vertical distance between nanoparticles and coil. To test this, samples of 15.7 μg were measured 'side up' and 'side down' on a the planar coil. An average signal increase of 10.4% was observed when the surface dried closest to the magnet was facing the planar coil.

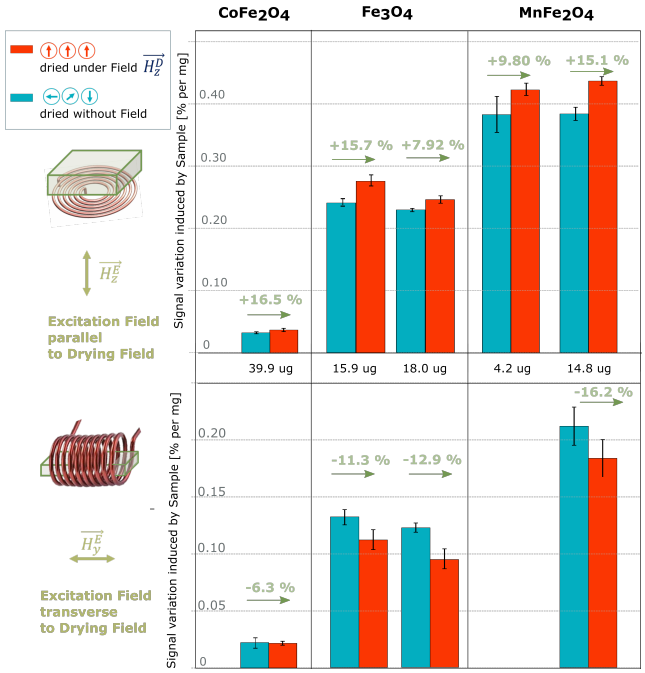

Fig. 3. Signal amplitude for different samples in both planar and wound coil. When EA are aligned parallel [transverse] to the excitation field through an external field during the drying process, signal amplitude is increased [decreased] with 6 to 16 %.

This confirms that drying in a magnetic field induces both EA orientation and a net displacement of the superparamagnetic nanoparticles (SPNs). This displacement is a minor but notable effect for distance-sensitive planar coil sensors, but dit not affect the wound coil measurements.

IV. Discussion and Perspectives

The difference between the 'best configuration' where EA orientation is parallel to the sensing field, and the worst in which both orientations are orthogonal, is over 31% for the 14.8 μg $MnFe_2O_4$ sample, which is significant for sensing applications. (1) Regardless of EA orientation, a clear distinction can be made in signal strength for the three materials, correlated with the magnetocrystalline anisotropy (Table I) : the lower the crystalline anisotropy (and thus magnetic energy barrier), the higher the directional susceptibility. (2) Based on the collected data, aligning the EA does not affect the sensed signal more for Fe_3O_4 than for $MnFe_2O_4$, confirming effective anisotropy is not only dominated by crystalline anisotropy, but also surface anisotropy [7]. (3) While the directional nature of the set-up clearly differentiates the contribution of pre-detection EA orientation, it was also demonstrated that an external drying field affects the clustering dynamics. The effects altered dipolar interactions on the effective anisotropy should be studied further.

Acknowledgment

The authors thank Ron Goldfarb, Yves Gossuin, Maria Salvador, Romain Hanus, Nicolas Roisin and Jose-Carlos Martinez-Garcia for fruitful discussions.

REFERENCES

[1] E. Martin, Y. Gossuin, S. Bals, S. Kavak, and Q. Lam Vuong, "Monte Carlo Simulations of the Magnetic Behaviour of Iron Oxide Nanoparticle Ensembles: Taking Size Dispersion, Particle Anisotropy, and Dipolar Interactions into Account" The European Physical Journal vol. B95, no. 12, December 2022, pp. 201.

[2] M. Salvador et al., "Improved Magnetic Lateral Flow Assays with Optimized Nanotags for Point-of-Use Inductive Biosensing" in The Analyst, vol. 145, no. 17, 2020, pp 5905–14.

[3] Egli, R. "Magnetic Susceptibility Measurements as a Function of Temeperature and Freqeuncy I: Inversion Theory" Geophysical Journal International 177, no. 2, May 2009, pp 395–420.

[4] Claudio Scherer and Hans-Georg Matuttis, 'Rotational Dynamics of Magnetic Particles in Suspensions'. Physical Review E 63, no. 1, December 2000, 011504

[5] H. Gavilan, K. Simeonidis, E. Myrovali, "How size, shape and assembly of magnetic nanoparticles give rise to different hyperthermia scenarios", Nanoscale vol. 13 2021, 15631–15646

[6] E. Myrovali , N. Maniotis, A. Makridis, A. Terzopoulou, V. Ntomprougkidis, K. Simeonidis, "Arrangement at the Nanoscale: Effect on Magnetic Particle Hyperthermia" Sci Rep vol. 6, no. 1, November 2016, pp 37934

[7] V. Pilati et al., "Mn-ferrite nanoparticles as promising magnetic tags for radiofrequency inductive detection and quantification in lateral flow assays" in Nanoscale Adv., vol. 6, 2024, pp 4247–58.

[8] E.F. Huda, S.I. Putri, "Tailored functional oxide nanomaterials: from design to multi-purpose applications" in Contemp. Phys vol. 63, no. 3, July 2022, pp243–244

[9] Kevin R. Minard, Matthew H. Littke, Wei Wang, Yijia Xiong, Justin G. Teeguarden, Brian D. Thrall, 'Magnetic Particle Detection (MPD) for in-Vitro Dosimetry'. Biosensors and Bioelectronics 43, May 2013, pp 88–93.